Interaction of the δ-Endotoxin CytA from *Bacillus thuringiensis* var. *israelensis* with Lipid Membranes

Peter Butko,*,‡ Fang Huang,§ Marianne Pusztai-Carey,|| and Witold K. Surewicz*,⊥

Institute for Biological Sciences, National Research Council of Canada, Ottawa, Ontario, Canada K1A 0R6, and Departments of Biochemistry and Pathology, Case Western Reserve University, Cleveland, Ohio 44106

Received January 31, 1997; Revised Manuscript Received August 13, 1997⊗

ABSTRACT: We investigated the binding of CytA, a cytolytic δ-endotoxin from *Bacillus thuringiensis* var. *israelensis*, to small unilamellar lipid vesicles (SUV) and the accompanying changes in the overall CytA conformation. From the titration of tryptophan fluorescence with SUV, we determined the apparent association constants of 3500 M^{-1} and 11000 M^{-1} for the protoxin CytA27 and the proteolytically activated toxin CytA24, respectively. Inclusion of a negatively charged lipid or a positively charged lipid analog in the membrane did not affect the binding parameters, which suggests that membrane binding is not driven by electrostatic interactions. A decrease in the intensity of the CytA tryptophan fluorescence upon interaction with lipids and the absence of a blue shift in remaining fluorescence indicate that the tryptophan-containing regions of the protein do not significantly penetrate into the hydrophobic core of the lipid bilayer. This finding was corroborated by the lack of additional quenching by brominated or spin-labeled lipids, irrespective of the location of the quenching moiety in the depth of the bilayer. However, the interaction with lipids decreases quenching with the soluble quenchers acrylamide and KI, and the remaining fluorescence is blue-shifted. The observed decrease in fluorescence anisotropy upon membrane binding is not consistent with simple immobilization of CytA on the surface of SUV. We showed by FTIR spectroscopy and differential scanning calorimetry (DSC) that binding to the membrane causes a significant loosening of the protein structure. This is consistent with the fluorescence quenching and anisotropy data. Our experiments provide evidence against CytA's substantially penetrating the lipid bilayer and creating well-defined proteinaceous channels.

The δ-endotoxins are a large family of proteins found in inclusion bodies of the bacterium *Bacillus thuringiensis* (*1*, *2*). They have been an object of interest due to their commercial potential as environmentally safe insecticides. CytA is a cytolytic δ-endotoxin produced by *B. thuringiensis* var. *israelensis* (*3*). CytA occupies a distinct place among the *B. thuringiensis* toxins. At least three characteristics make it very different from the rest of the family, the Cry proteins. First, CytA is smaller than any Cry protein. Second, its amino acid sequence shows very little homology to those of the other δ-endotoxins. Third, its cytolytic activity, which is enhanced upon proteolysis of the 27-kDa protoxin (CytA27) to the 24-kDa toxin (CytA24), is very broad (*4*, *5*) and not dependent on specific receptors on target cells. Nonspecific protein−lipid interaction as a part of the CytA mechanism of action was first suggested by Thomas and Ellar (*6*) and subsequently demonstrated in studies with multilamellar liposomes (*7*, *8*), planar lipid bilayers (*9*), and large and small unilamellar lipid vesicles (*10*). On the basis of observed changes in the planar bilayers conductivity upon addition of CytA, Knowles et al. (*9*) proposed that the protein acts by the formation of transmembrane ionic channels. However, features of secondary structure predicted from the amino acid sequence (*11*, *12*) do not contain any obvious hints as to the possible mechanism of transforming a soluble protein into a transmembrane channel. Due to the lack of data on the molecular organization and/or structure of putative channels, the current working model (*13*) remains hypothetical. Our present work provides some insights into conformational changes in CytA upon its interaction with the lipid membrane. Using a number of biophysical techniques, including fluorescence, CD, and Fourier-transform infrared (FTIR)[1] spectroscopies and DSC, we quantified CytA binding to the membranes and assessed the resulting conformational changes in CytA as well as the extent of CytA penetration into the membrane.

MATERIALS AND METHODS

Materials. Egg yolk L-α-phosphatidylcholine type V-E (egg PC)[1], stearylamine, NaCl, EDTA, and buffers were from Sigma Chemical Co. (St. Louis, MO). L-α-Dipalmitoylphosphatidylglycerol, 1-palmitoyl-2-oleoyl-*sn*-glycero-3-phospho-

* Address correspondence to P.B. or W.K.S.

‡ Present address: Channing Laboratory, Brigham and Women's Hospital, Harvard Medical School, 181 Longwood Avenue, Boston, MA 02115. Telephone: 1-617-525-0378. Fax: 1-617-731-1541. E-mail: pbutko@channing.harvard.edu.

§ National Research Council of Canada.

|| Department of Biochemistry, Case Western Reserve University.

⊥ Department of Pathology, Case Western Reserve University.

⊗ Abstract published in *Advance ACS Abstracts,* October 1, 1997.

[1] Abbreviations: 6−7BrPC, 1-palmitoyl-2-stearoyl(6−7)dibromo-*sn*-glycero-3-phosphocholine; 11−12BrPC, 1-palmitoyl-2-stearoyl(11−12)dibromo-*sn*-glycero-3-phosphocholine; CAPS, 3-(cyclohexylamino)-1-propanesulfonic acid; DSC, differential scanning calorimetry; EDTA, ethylenediaminetetraacetic acid; egg PC, egg yolk L-α-phosphatidylcholine; FTIR, Fourier-transform infrared; HEPES, *N*-(hydroxyethyl)-piperazine-*N*′-2-ethanesulfonic acid; HPLC, high-performance liquid chromatography; LUV, large unilamellar vesicles; NBD, nitrobenzoxadiazole; POPC, 1-palmitoyl-2-oleoyl-*sn*-glycero-3-phosphocholine; SDS−PAGE, sodium dodecyl sulfate−polyacrylamide gel electrophoresis; SEM, standard error of the mean; SUV, small unilamellar vesicles.

S0006-2960(97)00238-9 CCC: $14.00

choline (POPC), the brominated lipids 1-palmitoyl-2-stearoyl-(6−7)dibromo-*sn*-glycero-3-phosphocholine (6−7BrPC) and 1-palmitoyl-2-stearoyl(11−12)dibromo-*sn*-glycero-3-phosphocholine (11−12BrPC), and the spin-labeled lipid 1-palmitoyl-2-stearoyl-(16-doxyl)-*sn*-glycero-3-phosphocholine were from Avanti Polar Lipids, Inc. (Alabaster, AL). CytA was isolated from cultures of *B. thuringiensis* var. *israelensis* obtained from Institut Pasteur (Paris, France) as described before (*10*), using ion-exchange HPLC (*3*). The purity of the preparations was routinely checked by SDS−PAGE and occasionally by mass spectroscopy and N-terminal sequencing. The proteins were lyophilized and stored at −20 °C.

Vesicle Preparation. LUV are a better model of biological membranes than SUV; the former also bind CytA stronger than the latter (*10*). Yet, SUV were used for fluorescence spectroscopy in order to diminish light scattering in samples. Lipid (5 mg) in chloroform was dried under a stream of nitrogen. The resulting thin film of dried lipid was hydrated in 0.5 mL of buffer. The lipid suspension was vortexed and sonicated with a Sonifier 350 tip sonicator (Branson Sonic Power Co., Danbury, CT) at 4 °C for 20 min.

Steady-State Tryptophan Fluorescence. The measurements were performed with an SLM 8000C spectrofluorometer (Urbana, IL) equipped with a double monochromator and photon-counting detection system. The sample was thermostated at 20 °C and continuously stirred by a magnetic stirrer. Fluorescence was excited at 280 nm, and the emission was scanned from 300 to 400 nm. The spectra were corrected for dilution and for the instrument response. Unless stated otherwise, all the experiments were carried out in 100 mM NaCl, 10 mM HEPES, pH 7.4.

Anisotropy of tryptophan fluorescence was measured with the same fluorometer in the T format in a 3-mm path length quartz cell at 20 °C. Excitation and emission wavelengths were 295 and 340 nm, respectively. For the samples with lipid, egg PC SUV suspension (without the protein) was used as a blank. The data (each integrated for 2 s) were collected 40 times, and the average ± SEM was determined with the software provided by SLM. The protein and lipid concentrations were 690 nM and 1.44 mM, respectively.

Binding of CytA to the SUV. The proteins (1.7 μM and 1.2 μM for CytA27 and CytA24, respectively) were dissolved in a buffer (100 mM NaCl, and 10 mM HEPES or 50 mM CAPS or 50 mM citrate for pH 7.4, 10, or 4, respectively) and were titrated with egg PC SUV in a 3-mm path length quartz microcuvette. Aliquots of SUV suspension were added with a Hamilton syringe, and the cuvette contents were rapidly but thoroughly mixed by repeated aspiration into a Pasteur pipet. Titration of the fluorescence intensity with PC SUV was used to determine the binding parameters. The binding data were evaluated according to Bashford et al. (*14*) and Surewicz and Epand (*15*). The ratio K_d/n of the dissociation constant and stoichiometry is the reciprocal of the classic first association constant K_{app} for the protein−lipid interaction. Provided that $C_{L^o} \gg C_{P^o}$, K_d/n can be determined from the slope of the plot of $1 - F/F_o$ vs $(1 - F/F_o)/C_{L^o}$.

Quenching of Tryptophan Fluorescence. Fluorescence was measured in a 3-mm path length microcuvette with the same fluorometer. The excitation wavelength was 295 nm (in order to avoid the necessity of correction for a significant acrylamide absorption at 280 nm), and the emission wavelength was 335 nm. Protein concentrations were 2 μM for CytA27 and 2.3 μM for CytA24. Acrylamide was added from the 7.4 M stock solution. Quenching by KI was measured with the same setup, the fluorescence being excited at 280 nm. The ionic strength was kept constant by the Job method of continuous variation (*16*). Oxidation of iodide in the stock solution was prevented by adding a small amount of $Na_2S_2O_3$. The experimental data were fitted with the quenching equation:

$$F/F_o = f_1/(1 + K_1[Q]) + f_2/(1 + K_2[Q]) \qquad (1)$$

where F_o is fluorescence in the absence of quencher, F is fluorescence in the presence of quencher at the concentration [Q], and K_i are quenching constants associated with the respective fractions f_i of tryptophan fluorescence [see, e.g., Eftink (*16*)).

In addition to the aqueous quenchers, two kinds of lipidic quenchers were used: brominated lipids, 6−7BrPC and 11−12BrPC, where the quenching groups (bromine atoms) are located at two different positions along the lipid acyl chain, and a spin-labeled lipid, 1-palmitoyl-2-stearoyl-(16-doxyl)-*sn*-glycero-3-phosphocholine, which has the quenching doxyl group at the terminal carbon of the acyl chain. The protein concentration was 1.2 μM.

Egg PC SUV containing either 83 mol % of brominated lipids or 16 mol % of spin-labeled lipids were prepared as described above, with the quencher lipids predissolved with egg PC in chloroform.

Circular Dichroism (CD). CD spectra were measured with JASCO J-600 spectropolarimeter (Tokyo, Japan) in a 0.2-mm path length quartz cell. The buffer was 10 mM NH_4HCO_3, pH 8.5, which ensured good solubility of CytA. Eight scans were accumulated and averaged. The protein and, if present, lipid (egg PC SUV) concentrations were 7.4 μM and 3.3 mM, respectively, resulting in protein:lipid ratio of 1:445.

FTIR Spectroscopy. The protein (0.1 mg) was dissolved in 15 μL of D_2O buffered with 20 mM Tris, pD 9.3, and vortexed. When the presence of lipid was desired, 0.95 mg of POPC was dissolved in chloroform/methanol (3:1) and dried under nitrogen so that a lipid film was formed on the wall of an Eppendorf tube. Subsequently, the lyophilized protein and D_2O buffer were added, and the suspension was vigorously vortexed. The sample was sandwiched between two CaF_2 windows with a 50-μm Teflon spacer, and the infrared spectra were recorded with a Bio-Rad FTS 40A spectrometer (Cambridge, MA) equipped with a TGS detector. To eliminate the signal from atmospheric water vapor, the sample chamber was continuously purged with dry nitrogen and spectral contributions from residual water vapor were subtracted. The final protein spectra were obtained after spectral subtraction of the buffer and, where appropriate, lipid. The resolution was 2 cm^{-1}; 64 interferograms were accumulated and coadded. The peak positions were determined by the software provided by Bio-Rad.

The amide II proton/deuteron exchange was measured at room temperature (about 23 °C). In the thermal denaturation experiments, temperature was controlled with a Neslab RTE-110 refrigerated bath/circulator (Newington, NH) interfaced with the spectrometer's SPC 3200 data station. The data were collected automatically with software written by R. N. A. H. Lewis (Department of Biochemistry, University of Alberta, Edmonton, Alberta) and D. J. Moffat (Steacie

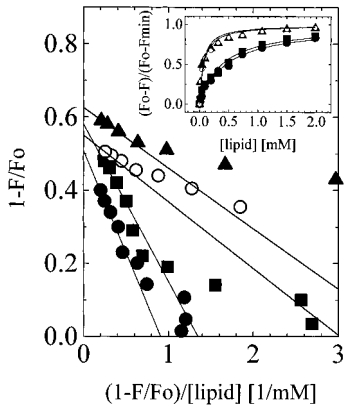

FIGURE 1: Binding of CytA27 (filled symbols) and CytA24 (open symbols) to egg PC SUV. CytA27 binding was measured at pH 7.4 (squares), 10 (circles), and 4 (triangles). Concentrations of the proteins were 1.7 and 1.2 μM for CytA27 and CytA24, respectively. Titration of the toxin fluorescence with lipid SUV is plotted as $1 - F/F_o$ vs $(1 - F/F_o)$/[lipid], where F_o and F are the fluorescence in the absence and presence of lipid, respectively. Straight lines indicate the initial slopes. Inset: Raw data with fitted hyperbolas (eq 2).

Institute for Molecular Sciences, National Research Council, Ottawa, Ontario).

Differential Scanning Calorimetry (DSC). A MicroCal MC-2 scanning calorimeter (Northampton, MA) was used in these experiments. Scan rates were 60 °C/h. The protein concentration was 0.7 mg/mL. For the samples with lipid, the walls of a vial were first covered with a POPC film (as described for FTIR samples), and the protein was hydrated together with lipid in 10 mM NH_4HCO_3, pH 8.5, by vortexing. The final lipid concentration was 7 mg/mL. A buffer profile was subtracted from the sample scans. Base lines were created by the cubic spline and subtracted. The calorimetric parameters T_m (midpoint temperature of the transition) and ΔH_{cal} (calorimetric enthalpy) were extracted from the data by the Origin software provided by MicroCal.

RESULTS

Binding of CytA to SUV Determined from Lipid-Induced Quenching of CytA Fluorescence. In the presence of 2 mM lipid, the fluorescence intensity of CytA decreased to 50%, and the maximum intensity wavelength was red-shifted from 335 nm by 2−5 nm in repeated experiments. The cause of this variation is not known. The decrease in intensity was well reproducible. Titration of the fluorescence intensity with PC SUV was used to characterize the protein binding to the membrane. Raw data are shown in the inset of Figure 1. We attempted to fit the data with the binding equation $KC_a^f = nr/(1 - nr)$, where K is the association constant, C_a^f is the concentration of free protein, n is the stoichiometry of binding (number of lipids per protein bound), and r is the mole fraction of bound protein to total lipid (*17*). The binding equation was transformed into the form containing directly measurable quantities, namely, the degree of binding x [defined as $(F_o - F)/(F_o - F_{min})$, where F_o is the initial intensity in the absence of lipid, F_{min} is the intensity in the presence of a saturating amount of lipid, and F is the intensity in the presence of a given amount of lipid], the total protein concentration C_{P^o}, and the corrected lipid concentration C_{L^o} (equal to 0.65 times the concentration of lipid in the cuvette, since only the fraction of 0.65 of total lipid in SUV is located in the outer monolayer of the vesicle membrane and is accessible for toxin binding):

$$C_{L^o} = nx\{C_{P^o} + 1/[K(1 - x)]\} \quad (2)$$

This equation was fitted to the data. However, our experience, and that of others (*18*), was that the fitting parameters K and n had large uncertainties and were correlated; i.e., one could widely vary both of them, while keeping the ratio constant, without adverse effect on the quality of fit. Therefore, we instead evaluated the binding data according to Bashford et al. (*14*) and Surewicz and Epand (*15*), as mentioned under Materials and Methods. This approach does not attempt to separate the association constant and stoichiometry (number of lipids per protein bound) as, for instance, Tamm and Bartoldus (*17*) did, but it yields a reliable indication of the overall affinity of a protein to the membrane. An advantage of this method is that it does not require knowledge of fluorescence intensity at saturation (i.e., infinite lipid concentration), which is necessary for definition of the binding parameter in the approach of Tamm and Bartoldus. Figure 1 depicts the plots of $1 - F/F_o$ vs $(1 - F/F_o)/C_{L^o}$. The data significantly deviate from a straight line at low lipid concentration [large $(1 - F/F_o)/C_{L^o}$], where the condition $C_{L^o} \gg C_{P^o}$ does not hold and, consequently, the model is not applicable. Only the initial slope was used to determine K_d/n and its reciprocal, K_{app}. The summary of binding constants is given in Table 1.

Table 1: Apparent Association Constant, K_{app}, for the Interaction between CytA and PC SUV at Different pHs[a]

system	K_{app} (M^{-1})
CytA27, pH 7.4	3500
CytA27, pH 10	3250
CytA27, pH 4	11000
CytA24, pH 7.4	11000

[a] K_{app} was determined from the initial slopes in Figure 1. For experimental conditions, see Figure 1.

Inclusion of 20 mol % of the negatively charged lipid dipalmitoylphosphatidylglycerol or the positively charged lipid stearylamine did not significantly change membrane binding of CytA27 at neutral pH (data not shown).

Fluorescence Anisotropy. Apart from the substantial change in the fluorescence intensity and the small red shift of the spectrum, the fluorescence anisotropy r also exhibited significant change in the presence of membranes. The values of r of the CytA27 fluorescence were 0.139 ± 0.003 and 0.104 ± 0.004 in the absence and presence of lipid, respectively.

Quenching of CytA Fluorescence. Since most of the Stern−Volmer plots were curved downward (not shown), we used a nonlinear least-squares method to fit eq 1 to the data (plots F/F_o vs [Q]). The second quenching constant K_2 was usually a small number (sometimes negative, which does not have physical meaning). We fixed its value at zero, thus making an assumption that a fraction of tryptophans is completely inaccessible to aqueous quenchers. The best fits of the quenching parameters (quenching constants and fluorescence fractions) are summarized in Table 2. Only in the case of acrylamide quenching of the CytA24 fluorescence was it sufficient to consider a single fraction of fluorescence quenched with a single quenching constant (i.e., $f_2 = 0$), which implies that the two tryptophans of CytA24 are equally

Table 2: Parameters of Quenching of the CytA Fluorescence by Acrylamide (AA) and KI[a]

quencher	system	K_1 (M^{-1})	f_1	K_{eff} (M^{-1})
AA	CytA24	7.8 ± 0.2	1.00	7.8 ± 0.2
AA	CytA24 + PC SUV	3.2 ± 0.1	1.00	3.2 ± 0.1
AA	CytA27	7.0 ± 0.3	1.00	7.0 ± 0.3
AA	CytA27 + PC SUV	8.0 ± 0.6	0.77 ± 0.03	6.2 ± 0.7
KI	CytA24	5.9 ± 0.8	0.75 ± 0.04	4.4 ± 0.8
KI	CytA24 + PC SUV	4.7 ± 0.5	0.57 ± 0.02	2.7 ± 0.4
KI	CytA27	6.3 ± 0.6	0.75 ± 0.02	4.7 ± 0.6
KI	CytA27 + PC SUV	4.6 ± 0.5	0.58 ± 0.02	2.7 ± 0.4

[a] The protein (2 μM and 2.3 μM for CytA27 and CytA24, respectively) was titrated by quencher in the absence (open symbols) and presence (filled symbols) of egg PC SUV (1.7 mM). The values were obtained by fitting eq 1 to the data. K_1 is the quenching constant associated with the fraction f_1 of total fluorescence. K_2 was fixed at zero and $f_2 = 1 - f_1$. The effective quenching constant $K_{eff} = \sum_i f_i K_i$.

accessible to acrylamide. The quenching pattern was more complex in the case of acrylamide quenching of the CytA27 fluorescence and KI quenching of both CytA24 and CytA27 fluorescence, where two fractions were necessary for satisfactory fits. The most reliable parameter is the effective Stern−Volmer quenching constant K_{eff} ($=\sum_i f_i K_i$). It depends the least on the assumed number and accessibility of tryptophan populations and the manner of data evaluation. The data in Table 2 show that the interaction of CytA with the membrane decreases quenching of tryptophan fluorescence, with the exception of acrylamide quenching of the CytA27 fluorescence, where the presence of lipid does not cause a significant drop in the value of K_{eff}.

Because of its charge, iodide has a greater selectivity for solvent-exposed fluorophores than acrylamide. Indeed, the iodide quenching profile suggests the existence of two different populations of tryptophans in CytA that have significantly different accessibility to the solvent. The fraction of nonquenched tryptophans in CytA27 increases in the presence of lipid (Table 2). Independent proof that the exposed and buried tryptophans experience physically different environments is offered by comparison of the positions of fluorescence maxima in quenched and unquenched samples. Fluorescence in the presence of 1.7 mM lipid and 1 M KI originates mostly from the inaccessible tryptophans, and its maximum occurs at 331 nm. The quenchable tryptophans exhibit an emission maximum at 337.2 nm, whereas the total protein fluorescence has its maximum at 335 nm. The blue shift in fluorescence of the nonquenchable tryptophans indicates that the latter are in a more hydrophobic environment, shielded from access from the aqueous phase. Similar but less pronounced shifts were observed with CytA24.

The apparent protection against quenching upon binding to the lipid may be steric—due to a direct shielding of the tryptophans by the membrane, or nonsteric—due to a decrease in the average fluorescence lifetime, caused by a conformational change in the protein. The possibility of direct insertion of the CytA molecule (or at least a part of it) was examined in the experiments with lipidic quenchers. If the tryptophans that are not accessible to aqueous quenchers are buried deep in the membrane bilayer, they should be readily quenchable by lipidic quenchers. We chose lipids with bromine as a quenching group located at a different depth in the lipid bilayer, at carbons 6, 7 and carbons 11, 12 in the lipid acyl chain. The experiments were performed 3 times, and all the data points fall within the SEM of the quenching by egg PC (data not shown). Similarly, no significant difference was observed between quenching by egg PC and the spin-labeled lipid with the quenching group on carbon 16 (data not shown). Thus, neither brominated lipids nor spin-labeled lipids enhanced quenching already caused by egg PC.

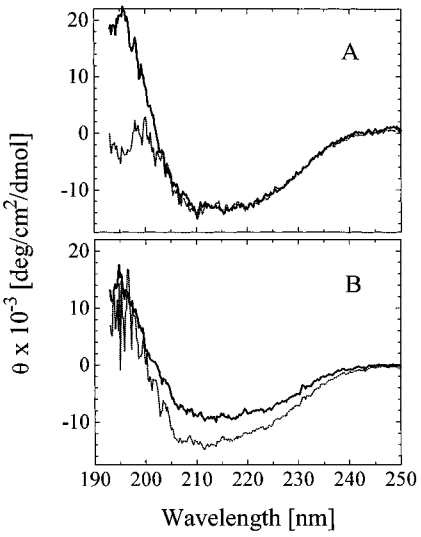

FIGURE 2: CD spectra of CytA27 (A) and CytA24 (B) in the absence (solid line) and presence (dotted line) of egg PC SUV. The protein and, if present, lipid concentrations were 7.4 μM and 3.3 mM, respectively, in a 10 mM NH_4CO_3 buffer, pH 8.5.

Circular Dichroism (CD). The CD spectra of both CytA27 and CytA24 in the absence and presence of lipid are shown in Figure 2. Large amounts of lipid had to be used in the sample in order to obtain a lipid-to-protein ratio favorable for protein binding. This produced significant light scattering that influenced the quality of the spectra, especially at wavelengths below 205 nm. Furthermore, high local concentration of the membrane-associated protein could potentially lead to artifactual flattening of the CD spectra (*19*). Therefore, the data were not band-fitted for quantitative analysis of protein secondary structure. Nevertheless, the spectra exhibit the same general shape. The presence of lipid apparently did not cause any significant changes in the secondary structure of CytA27. In CytA24, lipid binding seemed to induce some conformational change; the increase in negative ellipticity suggests somewhat more ordered secondary structure, but it is not possible to determine which structural element (α-helix or β-sheet) increased in content.

FTIR Spectroscopy. When a protein is hydrated in D_2O, protons in the amino acid side chains and the peptide-bond amide are exchanged for deuterons. The kinetics of this proton/deuteron exchange reflect accessibility of the protonated groups to the D_2O solvent: protons buried in the interior of the protein exchange more slowly, if at all, than those close to the surface of the protein. We measured the proton/deuteron exchange kinetics as the rate of disappearance of the amide II band. Our chosen parameter was the ratio of the intensity at 1541 cm^{-1} to the intensity of the amide I peak, which is approximately equivalent to the concentration normalization, since the intensity of the amide I peak does not change with time. The values of the amide II:amide I ratio as a function of time are depicted in Figure 3, together with exponential fits to the data. The ratio at

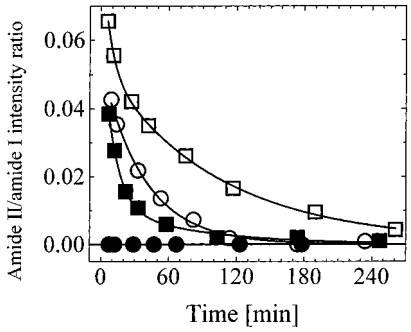

FIGURE 3: Kinetics of amide II proton/deuteron exchange. The measured parameter was the ratio of the infrared intensities at 1541 cm^{-1} and at the amide I peak (the 1640 cm^{-1} region). Open and filled symbols denote protein in the absence and presence of POPC multilamellar vesicles, respectively; squares and circles denote CytA27 and CytA24, respectively. The lines are exponential fits to the data (see text). The protein and lipid concentrations were 6.7 and 63.3 mg/mL, respectively.

time zero is not known since the first measurements were taken at 6 min. Although this precludes determination of exact kinetics, the following observations were made. The CytA27 data required two exponentials for a satisfactory fit, as judged by the 1 order of magnitude decrease in χ^2 with the second exponential. The average time constant t [calculated from the two individual constants t_i as $\sum_i t_i A_i / \sum_i A_i$, where A_i are the amplitudes in the sum of exponentials, $\sum_i A_i \exp(-x/t_i)$] decreased from 62 min in the absence of lipid to 24 min in its presence. The change in CytA24 is even more dramatic. In the absence of lipid, the CytA24 data after 6 min were well fitted with a single exponential with a time constant of 38 min. In the presence of lipid, even the first point was already indistinguishable from zero; i.e., all the amide II protons had already exchanged within the first 6 min. This implies a time constant of less than 4.3 min. Our results thus indicate a substantial loosening of the protein structure (increased exposure of the peptide backbone to the solvent).

That the structure of the protein was indeed loosened was confirmed by measurements of thermal stability of the protein. FTIR spectra were recorded at temperatures between 25 and 85 °C. In Figure 4, two parameters obtained from the spectra are plotted as a function of temperature: the appearance of a shoulder at 1615 cm^{-1} (Figure 4A), which is characteristic for thermal denaturation and irreversible aggregation of proteins (*20, 21*); and a shift in the position of the amide I maximum to higher wavenumbers (Figure 4B), which is indicative of increasingly irregular structure [band at 1646 cm^{-1} (*21*)]. Both plots show that in the absence of lipid, both proteins undergo a well-defined structural transition, with midpoint temperatures of about 49 and 54 °C for CytA27 and CytA24, respectively. The transitions in the presence of lipids are, however, extremely broad and shallow or even absent. It is interesting that the curves derived from the FTIR spectra do not start from the same point at 25 °C in the absence and presence of lipid. This suggests that binding to the membrane causes a significant change in the protein structure, similar to thermal unfolding. This finding is consistent with the results of the proton exchange experiments.

Differential Scanning Calorimetry. The most direct method for the assessment of thermal stability is DSC. The calorimetric profile of CytA27 is presented in Figure 5. In

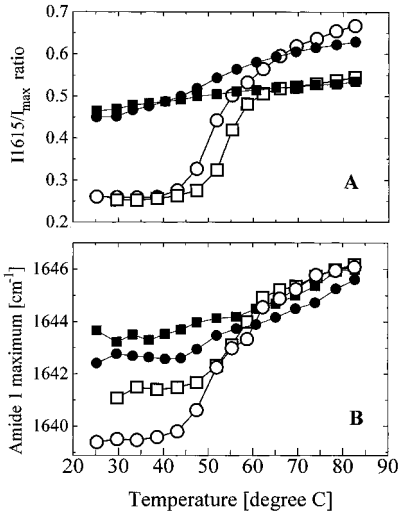

FIGURE 4: Thermal denaturation of CytA27 (circles) and CytA24 (squares) in the absence (open symbols) and presence (filled symbols) of POPC multilamellar vesicles determined by FTIR spectroscopy. The measured parameters were the ratio of the intensities at 1615 cm^{-1} and at the amide I peak (A) or the position of the amide I maximum (B). The protein and lipid concentrations were 6.7 and 63.3 mg/mL, respectively.

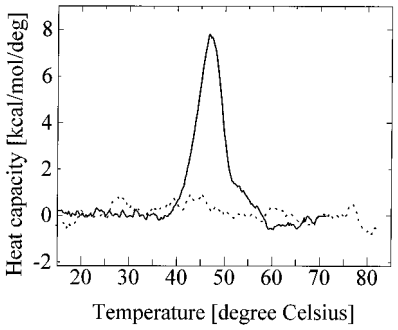

FIGURE 5: Thermal denaturation of CytA27 in the absence (solid line) and presence (dotted line) of POPC multilamellar vesicles determined by DSC. The protein and lipid concentrations were 0.7 and 7 mg/mL, respectively.

the absence of lipid, the protein unfolds at T_m = 46.7 °C with an enthalpy of 54.3 kcal/mol. Both of these values are relatively low, which suggests that the structure of CytA27 is not very rigid. No transition was observed in the second heating cycle of the same sample (data not shown), indicating that the unfolding is irreversible. DSC scans in the presence of lipid showed no detectable calorimetric transition in CytA (Figure 5).

DISCUSSION

Naturally occurring fluorescent amino acid tryptophan can be used as a probe to report changes in its local environment after or during interaction of a protein with the lipid membrane. CytA27 contains three tryptophans at positions 17, 158, and 161; after proteolysis, CytA24 retains the latter two (*22*). In general, tryptophans buried within a hydrophobic milieu exhibit higher a quantum yield of fluorescence, and the position of their emission maximum is blue-shifted when compared with the tryptophans accessible to solvent (*23, 24*). The quenching and slight red shift of CytA fluorescence upon interaction with lipids suggest that the CytA−lipid interaction is more complex than a simple insertion of the protein into the lipid bilayer. That the tryptophan-containing regions (the N terminus and putative

helix 3, amino acids 154−165) of CytA do not penetrate the bilayer to any significant extent was demonstrated by the lack of additional quenching by lipidic quenchers with the quenching moiety at various depths of the bilayer. Recently, Gazit and Shai (*25*) investigated membrane binding and permeabilization by two synthetic peptides mimicking putative helices 1 and 2 (amino acids 50−71 and 110−131, respectively) of CytA. The observation that the NBD-labeled helix 2 strongly interacted with lipids, aggregated in the membrane, and permeabilized the bilayer for ions led the authors to conclude that helix 2 (and to some extent also helix 1) participates in the pore formation by CytA. Due to the different location of our chosen intrinsic fluorescence probes, i.e., native tryptophans, we did not address directly the possible roles of helices 1 and 2 in the toxin's interaction with membranes. However, several points should be borne in mind when interpreting the results of Gazit and Shai (*25*). (i) The behavior of helical peptides may be quite different when they are in isolation and when they are part of the whole protein molecule where they engage in interactions with surrounding amino acids. (ii) Extrinsic labeling of peptides by a bulky NBD group may change their physicochemical properties, notably their partitioning in the membrane. (iii) The observed N-terminal NBD localization in the hydrophobic interior of the lipid bilayer by itself rules out the possibility that helix 2 spans the membrane. In the case of spanning, both the N- and C-termini have to be on the opposite surfaces of the membrane and, thus, in a polar environment. (iv) In an extensive site-directed mutagenesis study by Ward et al. (*22*), only one mutation in helix 2 out of three affected the CytA toxicity. By contrast, in helix 3, where two of our intrinsic probes are located, three out of four mutations had an effect, thus indicating that helix 3 is at least as important for the function of CytA as helix 2, if not more so. The above-mentioned points argue that our experiments with the whole native protein may bear more relevance to the biological activity of CytA than those with extrinsically labeled fragments of the molecule. Our results rule out the possibility of the insertion of helix 3 into the membrane. As discussed above, the data of Gazit and Shai do not support membrane spanning by helix 2. Helix 1 does not resemble a typical amphipathic helix in that its polar residues are not clustered on one side and also it lacks charged amino acids. Thus, the only helix that can possibly insert and span the membrane is helix 4. This possibility so far has not been investigated in sufficient detail.

Apart from fluorescence intensity, fluorescence anisotropy is another useful indicator of binding of proteins to lipid vesicles. When a protein becomes immobilized on the vesicle surface, its steady-state fluorescence anisotropy generally increases due to a restriction to the fluorophore's motion (*23*). It is interesting that the anisotropy of the CytA fluorescence does not increase after the addition of lipid, which would be expected upon simple binding and immobilization of the protein at the membrane surface. Quenching experiments were performed to address the question of the tryptophans' location in the lipid membrane. In the presence of SUV, the fluorescing tryptophans are less quenched with the water-soluble quenchers acrylamide and KI (Table 2). The relatively long wavelength of the fluorescence maxima indicates that the tryptophans are not buried in the lipid bilayer. The apparent reduction in accessibility to the quenchers may be the consequence of a decreased average fluorescence lifetime, or, possibly, of a steric hindrance due to the protein aggregation on the membrane. Although such aggregation has been invoked before (*10*, *25*, *26*), no direct and conclusive evidence exists. The lipid-induced decrease in fluorescence anisotropy and the red shift of the fluorescence maximum are both consistent with an enhanced flexibility and increased solvent exposure of tryptophans upon partial unfolding of CytA on the membrane.

Titration of fluorescence intensity was used for quantitative evaluation of the binding of CytA to the lipid membrane. We used the formalism of Bashford et al. (*14*), which yields the classic first association constant K_{app}. The following qualitative conclusions can be drawn from those experiments: (i) there is no difference in binding of the CytA27 to the membrane at pH 7.4 and pH 10; (ii) at pH 4, CytA27 binds the lipid about 3.5 times tighter than at neutral pH; (iii) at neutral pH, CytA24 binds the lipids about 3.5 times tighter than CytA27. We previously determined that the toxin is about 3 times more potent than the protoxin in releasing the contents of a lipid vesicle (*10*). Considering the present results, it seems likely that both forms of CytA act by the same mechanism and the difference in potency is solely due to the difference in binding. Lowering the pH increased both the rate constant for the protoxin-induced dye release from vesicles (*10*) and the binding affinity of the protoxin to lipids (Table 1). Similar pH dependency, observed for the activity of another δ-endotoxin from *B. thuringiensis*, CryIC, was attributed to increased hydrophobicity of the protein at low pH (*27*). It is possible that the same mechanism is operational in the case of CytA.

It is notable that the values of the association constants for SUV, measured herein by tryptophan fluorescence quenching (3.5×10^3 M^{-1} and 1.1×10^4 M^{-1} for CytA27 and CytA24, respectively), are 1 order of magnitude lower than those for LUV, determined previously from the dye leakage experiments (6.7×10^4 M^{-1} and 1.9 x 10^5 M^{-1}) (*10*). This is in accord with the previously reported difference in the CytA activity against SUV and LUV (*10*). The fact that the two results obtained by two completely different techniques lead to similar conclusions gives our work a certain degree of inner consistency.

We used FTIR spectroscopy to measure the rates of proton exchange between the peptide-bond amide and the solvent. The increase in the rates observed in the presence of lipid (Figure 3) lends further support to the notion that the protein remains on the surface of the membrane and does not partition in the lipid bilayer. If the latter were the case, the rate of exchange would decrease, rather than increase, due to the protection by lipid against access from the aqueous phase. In the case of CytA24, the lipid-induced acceleration of the proton exchange is so great that the exchange rate could not be measured. This result demonstrates that, upon binding to lipid, CytA changes its conformation such that the peptide-bond backbone of the protein becomes more accessible to the solvent. Yet, the circular dichroism measurements (Figure 2) indicate no appreciable changes in the secondary structure of CytA27 and, possibly, a small increase in the α-helix and/or β-sheet content in CytA24. We suggest that it is only the tertiary structure that is loosened upon lipid binding, while the bulk of secondary structure is retained, perhaps in a form similar to the so-called "molten globule" state (*28*, *29*). This hypothesis was

substantiated by measuring the thermal stability of CytA in the absence and presence of lipid. Whereas free protein undergoes well-defined thermal unfolding, no cooperative transition is seen in the presence of lipid (Figures 4 and 5). Similar destabilization and loss of cooperative transition upon binding to the membrane was observed for cytochrome c (*30*) and colicin (*31*). Gicquaud (*32*) also reported a complete disappearance of the calorimetric enthalpy of actin upon binding to lipid vesicles.

In summary, this work provides evidence for substantial structural changes in CytA upon binding to the lipid membrane. The protein loosens its tertiary structure while retaining most of its secondary structure. Our data are consistent with the notion that the protein unfolds on the membrane surface with little, if any, penetration into the lipid bilayer. These findings have important implications for understanding the mechanism by which CytA exerts its lytic action. Given our results, the notion that CytA acts by forming classical proteinaceous ion channels, in which the protein spans the lipid bilayer, is unlikely. The evidence rather points toward a general, detergent-like perturbation caused by CytA on the membrane surface. We note that this mechanism still does not rule out creation of pores, as is documented in the case of annexins (*33*), which do not span the bilayer and yet selectively transfer calcium, probably through the underlying faults in membrane structure. The putative CytA-induced channels or pores suggested by the experiments with black lipid membranes (*9*) may only be transient and occur just during the first contact of CytA with the membrane and the protein rearrangement. Schwarz and Robert (*34*) argue that a single pore with an area of 0.3 nm^2 and a lifetime of 15 ms would be sufficient to completely deplete the vesicle of its contents. The present data do not enable us to offer the final model, but we are convinced that our findings are pertinent for the future elucidation of the physiological mechanism of action of CytA and, conceivably, other δ-endotoxins.

REFERENCES

1. Hofte, H., and Whiteley, H. R. (1989) *Microbiol. Rev. 53*, 242−255.
2. Lereclus, D., Delecluse, A., and Lecadet, M. (1993) in *Bacillus thuringiensis, an Environmental Biopesticide: Theory and Practice* (Entwistle, P. F., Cory, J. S., Bailey, M. J., & Higgs, S., Eds.) pp 37−69, John Wiley & Sons, London, England.
3. Chilcott, C. N., and Ellar, D. J. (1988) *J. Gen. Microbiol. 134*, 2551−2558.
4. Knowles, B. H., and Ellar, D. J. (1987) *Biochim. Biophys. Acta 924*, 509−518.
5. Thomas, W. E., and Ellar, D. J. (1983a) *J. Cell Sci. 60*, 181−197.
6. Thomas, W. E., and Ellar, D. J. (1983b) *FEBS Lett. 154*, 362−368.
7. Drobniewski, F. A., and Ellar, D. J. (1988) *Biochem. Soc. Trans. 16*, 38−40.
8. Haider, M. Z., and Ellar, D. J. (1989) *Biochim. Biophys. Acta 978*, 216−222.
9. Knowles, B. H., Blatt, M. R., Tester, M., Horsnell, J. M., Carroll, J., Menestrina, G., and Ellar, D. J. (1989) *FEBS Lett. 244*, 259−262.
10. Butko, P., Huang, F., Pusztai-Carey, M., and Surewicz, W. K. (1996) *Biochemistry 35*, 11355−11360.
11. Waalwijk, C., Dullemans, A. M., van Workum, M. E. S., and Visser, B. (1985) *Nucleic Acids Res. 13*, 8207−8217.
12. Ward, E. S., and Ellar, D. J. (1986) *J. Mol. Biol. 191*, 1−11.
13. Gill, S. S., Cowles, E. A., and Pietrantonio, P. V. (1992) *Annu. Rev. Entomol. 37*, 615−636.
14. Bashford, C. L., Chance, B., Smith, J. C., and Yoshida, T. (1979) *Biophys. J. 25*, 63−85.
15. Surewicz, W. K., and Epand, R. M. (1984) *Biochemistry 23*, 6072−6077.
16. Eftink, M. R. (1991) in *Biophysical and Biochemical Aspects of Fluorescence Spectroscopy* (Dewey, T. G., Ed.) pp 1−41, Plenum Press, New York.
17. Tamm, L. K., and Bartoldus, I. (1988) *Biochemistry 27*, 7453−7458.
18. McLaughlin, S., and Harary, H. (1976) *Biochemistry 15*, 1941−1948.
19. Mao, D., and Wallace, B. A. (1984) *Biochemistry 23*, 2667−2673.
20. Jackson, M., Mantsch, H. H., and Spencer, J. H. (1992) *Biochemistry 31*, 7289−7293.
21. Fabian, H., Schultz, C., Naumann, D., Landt, O., Hahn, U., and Saenger, W. (1993) *J. Mol. Biol. 232*, 967−981.
22. Ward, E. S., Ellar, D. J., and Chilcott, C. N. (1988) *J. Mol. Biol. 202*, 527−535.
23. Lakowicz, J. R. (1983) *Principles of Fluorescence Spectroscopy*, Plenum Press, New York.
24. Phillips, W. J., and Cerione, R. A. (1991) in *Biophysical and Biochemical Aspects of Fluorescence Spectroscopy* (Dewey, T. G., Ed.) pp 135−167, Plenum Press, New York.
25. Gazit, E., and Shai, Y. (1993) *Biochemistry 32*, 12363−1237.
26. Maddrell, S. H., Overton, J. A., Ellar, D. J., and Knowles, B. H. (1989) *J. Cell Sci. 94*, 601−608.
27. Butko, P., Cournoyer, M., Pusztai-Carey, M., and Surewicz, W. K. (1994) *FEBS Lett.* 340, 89−92.
28. Ptitsyn, O. B., Pain, R. H., Semisotnov, G. V., Zerovnik, E., and Razgulyaev, O. I. (1990) *FEBS Lett. 262*, 20−24.
29. van der Goot, F. G., Lakey, J. H., and Pattus, F. (1992) *Trends Cell Biol. 2*, 343−348.
30. Muga, A., Mantsch, H. H., and Surewicz, W. K. (1991) *Biochemistry 30*, 7219−7224.
31. Muga, A., Gonzalez-Manas, J. M., Lakey, J. H., Pattus, F., and Surewicz, W. K. (1993) *J. Biol. Chem. 268*, 1553−1557.
32. Gicquaud, C. (1993) *Biochemistry 32*, 11873−11877.
33. Demange, P., Voges, D., Benz, J., Liemann, S., Gottig, P., Berendes, R., Burger, A., and Huber, R. (1994) *Trends Biochem. Sci. 19*, 272−276.
34. Schwarz, G., and Robert, C. H. (1992) *Biophys. Chem. 42*, 291−296.

BI9702389